

Stress-whitening of micro-composite thermoplastics

KASAJIMA, Masayuki / 小井戸, 正六 / 伊藤, 勝彦 / 笠島, 正行 / KOIDE, Shoroku / ITO, Katsuhiko

(出版者 / Publisher)

法政大学工学部

(雑誌名 / Journal or Publication Title)

Bulletin of the Faculty of Engineering, Hosei University / 法政大学工学部
研究集報

(巻 / Volume)

8

(開始ページ / Start Page)

17

(終了ページ / End Page)

32

(発行年 / Year)

1972-03

(URL)

<https://doi.org/10.15002/00004229>

STRESS-WHITENING OF MICRO-COMPOSITE THERMOPLASTICS

Masayuki KASAJIMA, *Assistant*
Katsuhiko ITO, *Professor*
Shoroku KOIDO, *Professor*

Abstract

This paper exhibits two subjects: one is the experimental results of macroscopic relationship between the stress-whitening (the stress crazing) and mechanical properties, and between the stress-whitening and the dielectric constant with respect to High Impact Polystyrene being one of micro-composite thermoplastics; other is theoretical analyses of relationship between quantity of the craze and the bending elastic modulus under the condition of presuming the matrix and the craze as an elastic body, and of utilizing simplified model.

I. Introduction

When high polymer materials such as modified rubber, so-called micro-composite thermoplastics, High Impact Polystyrene (HI-PS) resin and ABS resin are stressed, an opaque whitening phenomenon occurs at a certain stress value. This phenomenon is so-called stress-whitening. It has been described as a craze^{1~5)}, not a crack. The craze does not consist of void, but of craze-matters orientating at right angle to the major axis of the craze. The major axis of the craze agrees with direction of right angle to the stress. It has been thought that such stress-whitening is highly localized. C.B. Bucknall and R.R. Smith⁶⁾ think that the presence of rubber makes apt to occur such crazing. The reason is that High Impact Polystyrene is tougher than Polystyrene (PS) resin. R.P. Kambour^{7),8)} describes the craze as being orientated-matrix itself and elastic modulus of the craze being lower than the value of the matrix's, nevertheless it behaves as an elastic body.

Therefore, with the thought that the crazed portion (the portion occurring the stress-whitening) is elastic, this paper is a report on the results of investigation of macroscopic relationship between the stress-whitening (the stress-crazing) and mechanical properties, and between the stress-whitening and dielectric constant with respect to HI-PS by actual experiments, and the results are given of theoretical investigation with a simplified model of the relationship between quantity of the craze and bending elastic modulus.

II. Test Specimen and Experimental Methods

1. *For Investigation of Relationship between Stress-Whitening and Tensile, Bending Properties*

For test specimen, TOPOREX 830 sheet, 1 mm thick, manufactured by Mitsui-Toatsu Kagaku Co., Ltd., was used. This product is a HI-PS containing rubber to improve resistance to impact.

To investigate the relationship between the mechanical properties of the material

and the stress-whitening, it is desirable that the stress-whitening is distributed uniformly over the specimen. To achieve this object and to allow macroscopic observation of the occurrence of the craze, the stress-whitening is brought about by applying a tensile load. The tensile specimen is dumb-bell in shape. Mechanical properties of the specimens were measured before and after the stress-whitening by a simple support bending test. The bending specimen was a rectangular plate. In these tension and bending tests, an Instron type universal Auto-Graph IS-2000 made by Shimadze Seisaku-sho, Ltd., Kyoto, was utilized. In this paper, the nominal value is used for the value of tensile stress in the tension test. The HI-PS of the specimen is tough and does not fracture in bendable region. Therefore, bending strength is calculated from the following expression:

$$S = \frac{3Pl}{2wt^2}$$

Where S = bending strength, kg/mm^2
 P = maximum load in bending load-deflection curve given by bending test, kg
 l = distance between fulcrums, mm
 w = width of the specimen, mm
 t = thickness of the specimen, mm

2. For Repeating Test for Bending and Elimination of Stress-Whitening

For the test specimen, HI-PS TOPOREX 830 sheet, 1 mm thick, as used in the preceding section, was used. The stress-whitening which had occurred disappeared when the specimen was heated over the glass transition temperature. Therefore, for investigation of mechanical properties of the specimen in which the stress-whitening disappeared, the following tests were performed.

When bending test was performed by Auto-Graph IS-2000, the stress-whitening occurred in the portion of the specimen pressed by loading wedge of the bending apparatus. The bending specimen was a rectangular plate cut out of a bigger piece of the matrix. After the bending test, the stress-whitened portion of the specimen was heated over the glass transition temperature in an electric heating furnace to eliminate the stress-whitening. In this test, the stress-whitening was eliminated at 100°C . By alternately bending and eliminating the stress-whitening, one obtains the relationship between the bending strength and number of times for bending.

3. To determine Relationship between Stress-Whitening and Dielectric Constant

For the test specimen, an HI-PS is a rubber modified to improve its resistance

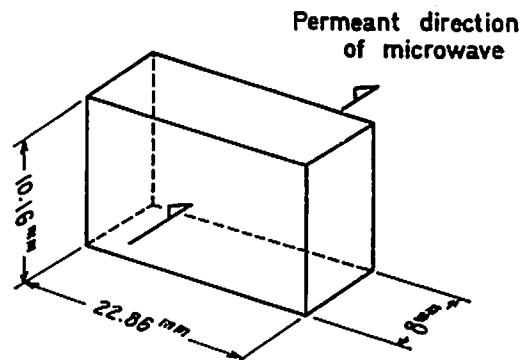


Fig. 1 Geometry of specimen for dielectric constant measurement.

to impact, bar of so-called TOPOREX 850, manufactured by Mitsui-Toatsu Kagaku Co., Ltd., Tokyo, was used.

To determine the dielectric constant of material occurred the stress-whitening, a tensile load was applied to a tensile specimen of dumb-bell type until the stress-whitening occurred. An Auto-Graph IS-2000, as used in the preceding test, was used for applying the tensile load. The dielectric constant of the specimen was measured before and after the stress-whitening occurred by microwave measurement method⁹⁾. The geometry of the specimen for the dielectric constant measurement is shown in Fig. 1. In this measurement, the instrument indicated in Fig. 2 was utilized. The utilized microwave was 9375 MHz.

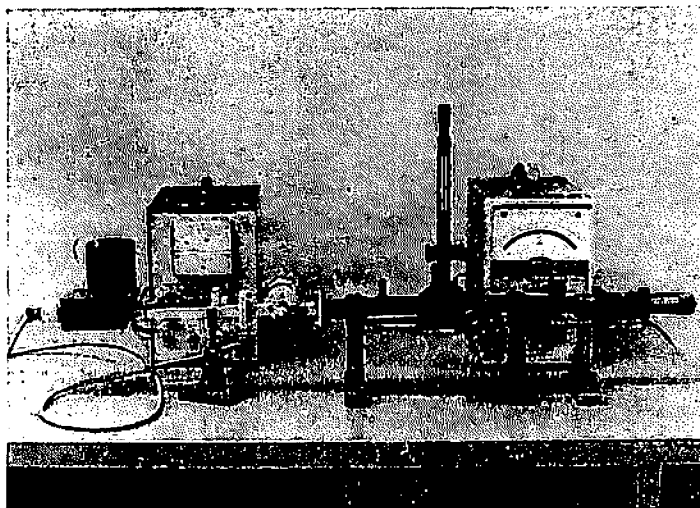


Fig. 2 Microwave-dielectric constant measuring instrument.

III. Experimental Results

1. Stress-Whitening under Tensile Load

To determine the relationship between tensile strain and the stress-whitening, tension tests were performed. A specimen in which the stress-whitening was brought about by tension is shown in Fig. 3. In this figure, it is recognized clearly that most of the crazing runs at right angles to the direction of tensile stress. Fig. 4 is an electron microscopic photograph which shows a microscopical part of the major axis of the craze in Fig. 3. From Figs. 3 and 4, it can be seen that the stress-whitening consists of many crazes and individual craze can not be found with the naked eye.

The results of stress-strain curve are shown in Figs. 5 and 6. The curve in Fig. 5 displays an average of the data. In Fig. 5, the stress-whitening can be observed near the limit of elasticity, point (2). As the tensile strain increases over the upper yield point (3), the area of stress-whitening expands and the stress-whitening deepens with increase in strain, and if the strain continues to increase, the specimen cracks and fractures. Growth of the stress-whitening (the craze) becomes remarkably clear with increase in strain. In Fig. 6, the major axis of the craze becomes longer and bigger with increase in strain. Moreover, with the strain increasing, among the major axes of the craze are filled in the craze itself, the stress-whitening expands and deepens all the more. Thus, the specimen becomes completely milky in colour as (6) in Fig. 6 and the major axis of each craze can not be discriminated with the naked eye.

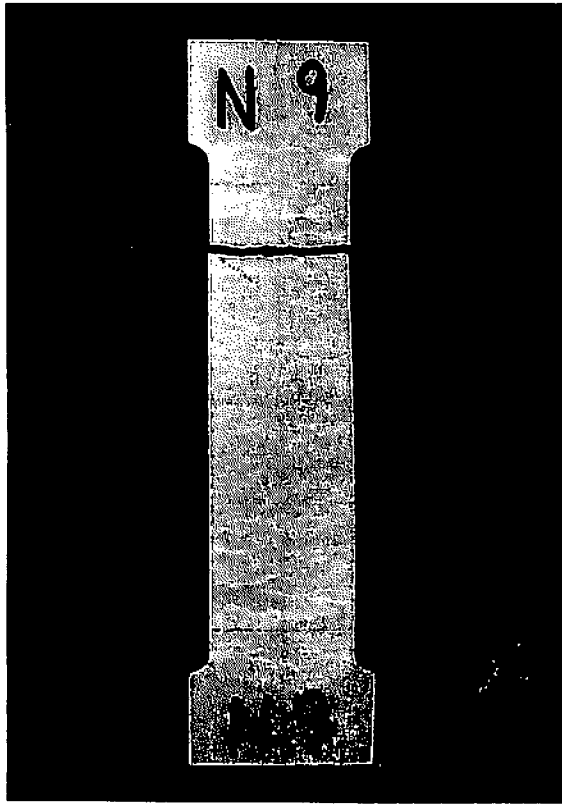


Fig. 3 Specimen with stress-whitening occurred by tension applying in major axis direction.

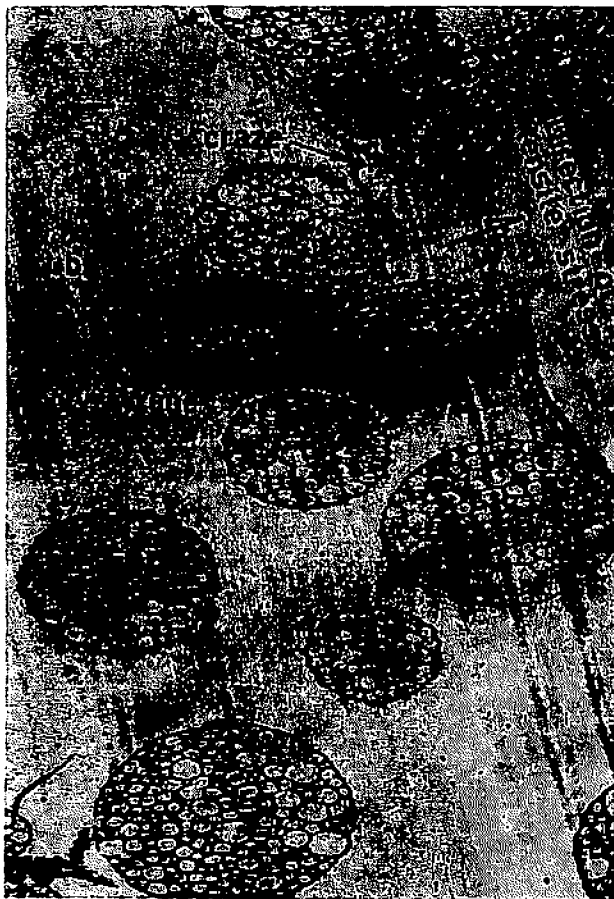


Fig. 4 Electron microscopic photograph ($\times 10,000$) of HI-PS, TOPOREX 830-02.

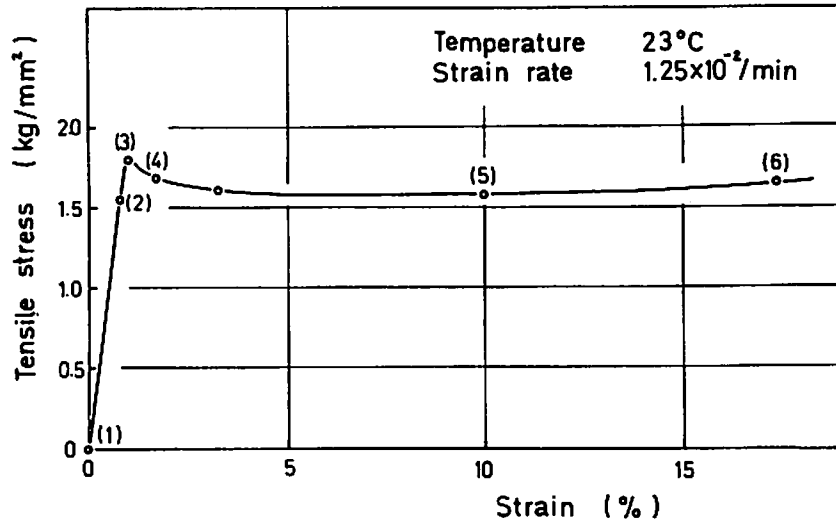
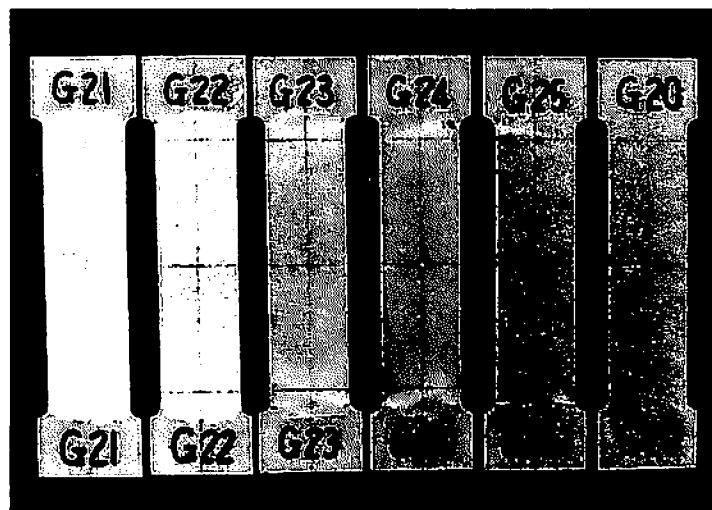


Fig. 5 Tensile stress-strain curve.

Fig. 6 Relationship between stress-whitening and tensile strain at 23°C, strain rate 1.25×10^{-2} /min.

Tensile stress-elongation curves showing the relationship between the stress-whitening and temperature under various temperatures is shown in Fig. 7. The photographic results of the test are exhibited in Fig. 8. It is shown Fig. 7 that the yield point rises with decrease in temperature and sensitive rate of the stress-whitening becomes also larger. That sensitive rate of the stress-whitening is large is that the orientated craze-matter becomes more with decrease in temperature at identical strain and deep of the stress-whitening becomes also deeper. In Fig. 8, many major axes of the craze can be observed with increased in temperature, i.e., the stress-whitening of the specimen at lower temperature is deeper. Hence, these figures indicate that temperature is also a factor in the stress-whitening. The stress-whitening does not occur at 100°C which is over the glass transition temperature.

As above, consequently, it seems that the stress-whitening can be represented qualitatively by parameters of strain, stress and temperature.

2. Relationship between Stress-Whitening and Bending Strength

For comparing bending strength of specimens before and after stress-whitening,

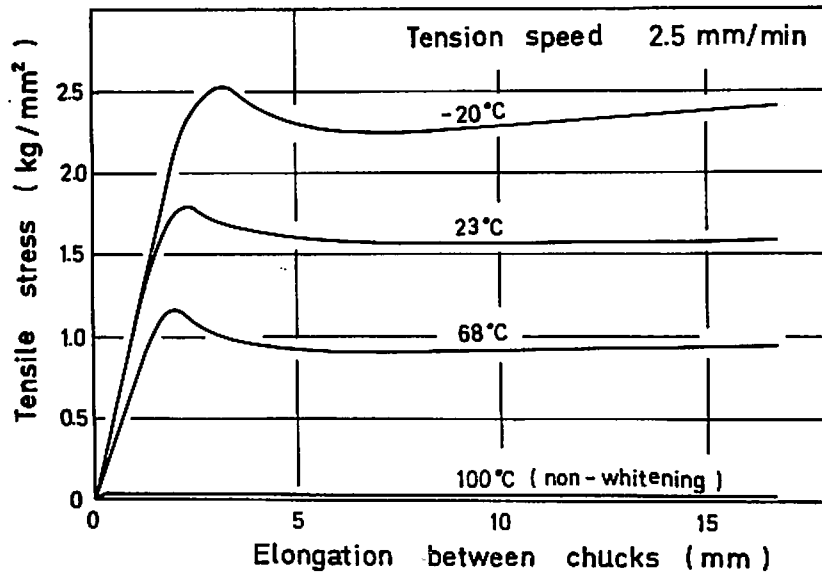


Fig. 7 Tensile stress-elongation curves under various temperatures.

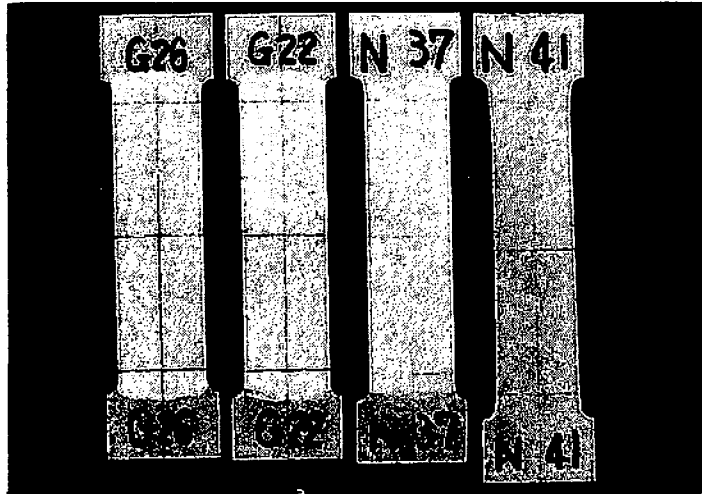


Fig. 8 Relationship between stress-whitening and temperature at tensile strain 10%, tension speed 2.5 mm/min.

the relationship between the bending strength of the matrix and temperature is shown in Fig. 9. The figure shows that the bending strength becomes smaller with increase in temperature. The bending strength at 100°C is extremely small in comparison with the value at lower temperature than 90°C. Consequently, the bending strength of the matrix decreases in straight line with increase in temperature as far as 90°C.

Bending test specimens as shown in Fig. 10 were extracted from the specimens shown in Fig. 6. The results of the bending tests are exhibited in Fig. 10. In the tensile test, the upper limit of tensile strain is in the neighbourhood of 18%. Therefore, the values of the bending strength are measured as far as 18% tensile strain. The figure shows that the bending strength value (S_{\parallel}) in direction of the tensile stress is lower than the value (S_{\perp}) perpendicular to the stress. The bending strength decreases with increase in the tensile strain. Comparing the strength values obtained with bending in direction of the tensile stress with those obtained with bending perpendicular to the direction of tensile stress, it is noted that the bending strength S_{\parallel}

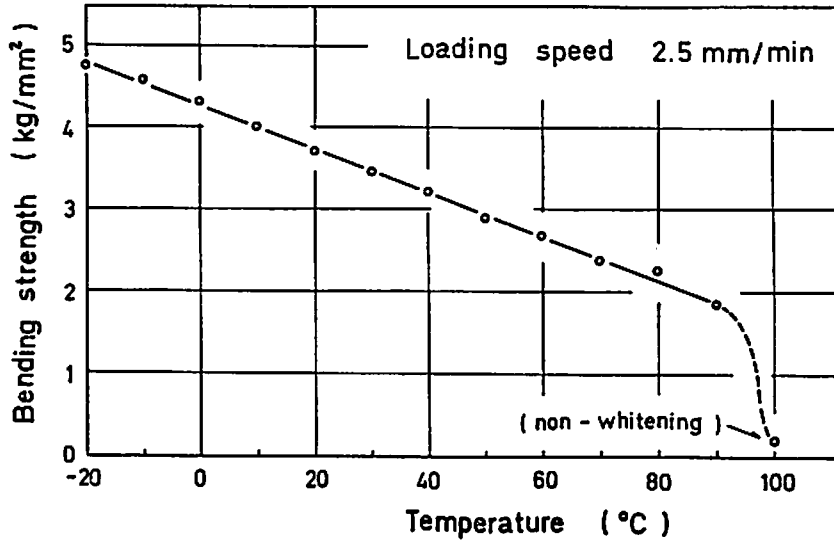


Fig. 9 Bending strength of matrix vs. temperature.

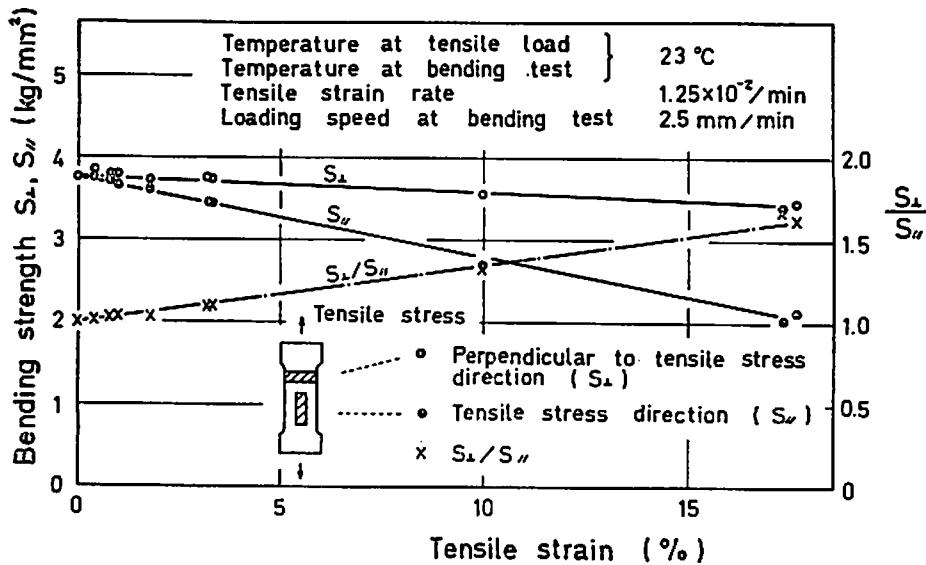


Fig. 10 Bending strength vs. tensile strain, and anisotropy defined as S_{\perp}/S_{\parallel} .

of the specimen in the tensile stress direction decreases more than the value S_{\perp} of perpendicular to the stress direction. This indicates that the bending strength decreases in straight line with increase in the tensile strain, i.e., quantity of stress-whitening or craze.

R.P. Kambour^{7),9)} says that the craze is an orientated-matrix itself and that though the elastic modulus of the craze is lower than the value of the matrix's, nevertheless it behaves as an elastic body. Hence, thinking a schematic simplified bending specimen model as shown in Fig. 11 instead of the bending specimen in Fig. 10, it is apt to understand that S_{\perp} is larger than S_{\parallel} . In Fig. 11, the specimen of (a) is a sandwich structure in which the matrices (elastic modulus E is large) and the crazes (elastic modulus E is small) are arranged at equal intervals from each other in direction of the major axis of the specimen, (b) is a sandwich structure in which the matrices (E : large) and the crazes (E : small) are arranged at equal intervals from each other in direction of perpendicular to the major axis of the specimen. Comparing specimens (a) and (b), it is evident that the bending

strength of (a) is larger than that of (b). The relationship between the bending strength and temperature at tensile load is indicated in Fig. 12. Specimens of the bending test as shown in Fig. 12 are extracted from specimens shown in Fig. 8. The results of the bending test for their specimens are exhibited in Fig. 12. The figure indicates that the bending strength increases in straight line with increase in temperature at tensile load. The strength of a specimen extracted from the tensed specimen at 100°C proved to be the same as the matrix strength.

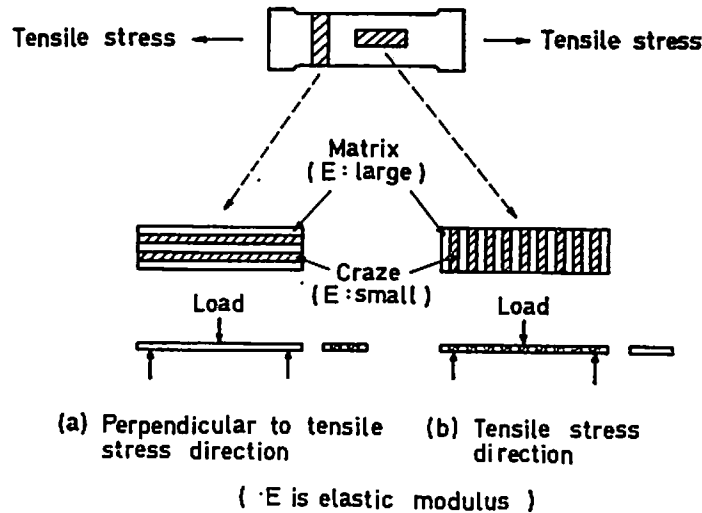


Fig. 11 Schematic simplified bending specimen model.

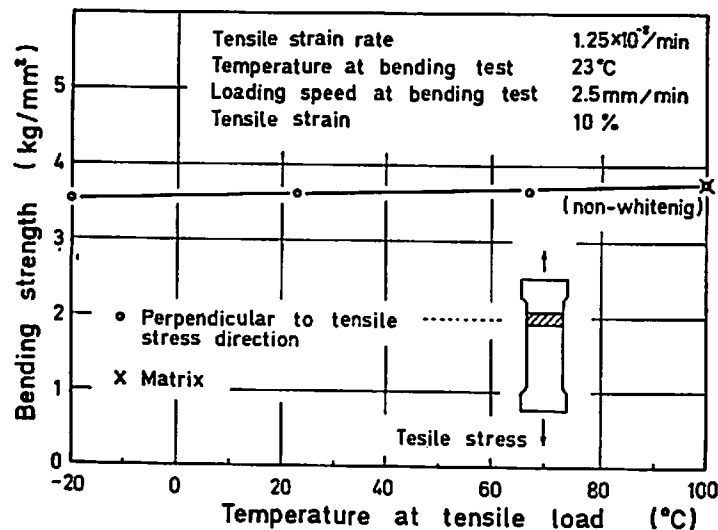


Fig. 12 Bending strength vs. temperature at tensile load.

3. Anisotropy under Bending Strength^{10), 11)}

The results of investigation of anisotropy defined as S_{\perp}/S_{\parallel} is shown in Fig. 10. The figure indicates that the anisotropy increases in straight line with increase in quantity of the stress-whitening, because the anisotropy under the bending strength increases in straight line with increase in the tensile strain. Where the tensile strain is 17.3%, the value of S_{\perp}/S_{\parallel} is approximately 1.6, i.e., it is about 1.6 times as large as the value of the matrix.

4. Repeating Test for Bending and Elimination of Stress-Whitening

The results of the repeating test for bending and elimination of the stress-whitening are shown in Fig. 13. The figure indicates that a crack occurs when the number of times for bending is in the neighbourhood of 16. Until a crack occurs, the bending strength stays at a constant value regardless of the number of times the specimen is bent and the strength stays the same as that of the matrix. This indicates that stress-whitened specimen recovers the same bending strength as the matrix's by heating over the glass transition temperature. If the cracked specimen is heated over the glass transition temperature, the stress-whitening surrounding the crack disappears. However, the crack itself does not disappear, and the bending strength of the cracked specimen decreases sharply. If the cracked specimen is subjected to bending and elimination of the stress-whitening alternately 3 to 5 times, the cracked specimen finally fractures.

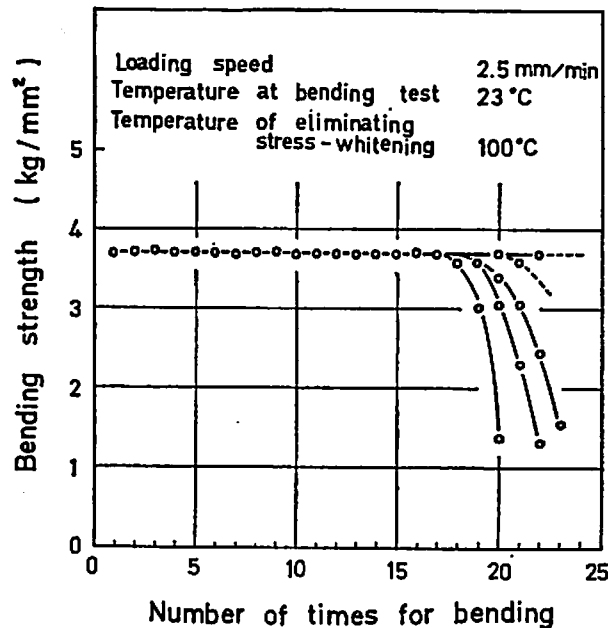


Fig. 13 Bending strength vs. number of times for bending.

5. Relationship between Stress-Whitening and Dielectric Constant

The results of the tests on the relationship between stress-whitening and dielectric constant are shown in Fig. 14. In this test, the elongation at tensile load is used as a parameter of the stress-whitening. The figure shows that the values of dielectric constant of the matrix (\times mark) are about 2.48~2.55 and the values of the specimens (\circ and \bullet) after stress-whitening has been increased by applying the tensile load are about 2.50~2.56. Consequently, the values of dielectric constant of the matrix and of the stress-whitened specimen differ hardly at all. The values of dielectric constant of the specimens extracted in respective direction from the tensile specimen as shown in Fig. 14 also show almost no difference.

IV. Theoretical

In this section, the results of investigation of the relationship between quantity of the craze and the bending elastic modulus are proposed. The analysis of the mechanical strength of the actual specimen is very complex. Therefore, if a

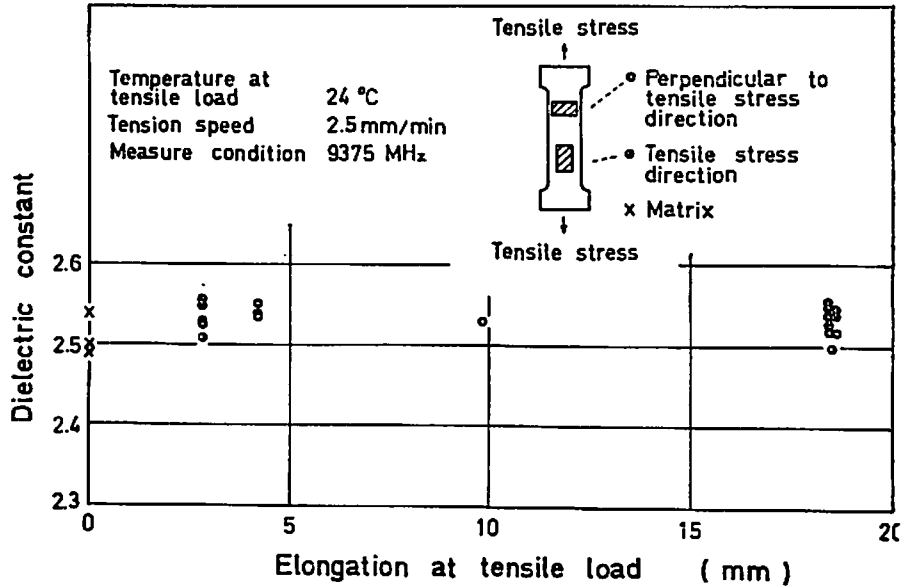


Fig. 14 Dielectric constant vs. elongation at tensile load.

schematic simplified model is used, the theoretical analyses of the mechanical strength are simplified greatly. Consequently, the bending strength was used in the experiment, however, the bending elastic modulus is employed in the theoretical analyses.

1. Bending in Direction Parallel to Major Axis of Craze

A schematic bending specimen model in the direction parallel to the major axis of the craze as shown in Fig. 15 is discussed. It is assumed that: the matrix and craze are arranged at equal intervals from each other; their numbers are respectively k_b ; quantity of craze is ξ ; bending elastic modulus of the matrix is ${}_mE_{bp}$; bending elastic modulus of the craze is ${}_cE_{bp}$; thickness of specimen is t ; and width of specimen is w . In Fig. 15, if a bending specimen in the direction parallel to the major axis of the craze is given pure bending moment M_p , the radius of curvature ρ results. For a sandwich structure specimen which is constituted with crazes and matrices as shown in Fig. 15, assuming that radii of curvature at respective boundaries of the craze and matrix is equal, the relationship between M_p and ρ is:

$$M_p = \frac{k_b}{\rho} ({}_mE_{bp} {}_mI_p + {}_cE_{bp} {}_cI_p) \tag{1}$$

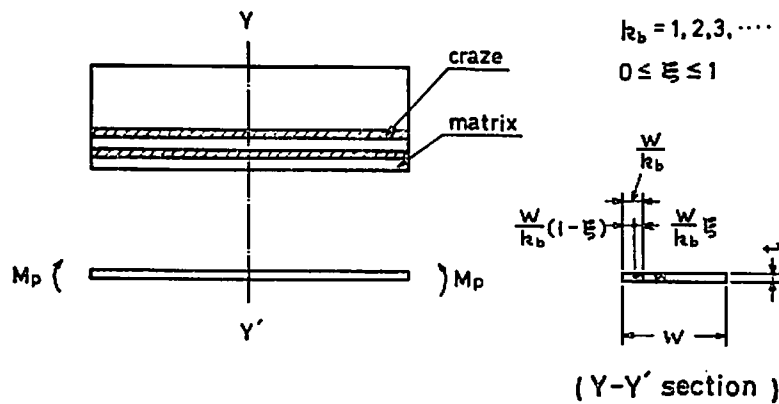


Fig. 15 Schematic bending specimen model in direction parallel to major axis of craze.

where the geometrical moment of inertia of the matrix and the craze are respectively:

$${}_m I_p = \frac{t^3}{12} \frac{w}{k_b} (1 - \xi), \quad {}_c I_p = \frac{t^3}{12} \frac{w}{k_b} \xi \quad (2)$$

If, in place of the sandwich structure specimen a unitary structure having elastic modulus E_{bp} and geometrical moment of inertia I_p is used, M_p of the unitary structure is:

$$M_p = \frac{1}{\rho} E_{bp} I_p, \quad \text{where } I_p = \frac{t^3}{12} w \quad (3)$$

The following expression is obtained from Eqs. (1), (2) and (3):

$$\frac{E_{bp}}{m E_{bp}} = 1 + \left(\frac{1}{\phi_p} - 1 \right) \xi, \quad \phi_p \equiv \frac{m E_{bp}}{c E_{bp}} \quad (4)$$

The relationship between $E_{bp}/m E_{bp}$ and ξ is shown in Fig. 16. In this graph, values of $E_{bp}/m E_{bp}$ decrease in straight line with increase in ξ and decreased-tendency of $E_{bp}/m E_{bp}$ values becomes larger with increase in value of ϕ_p . Though $\phi_p = \infty$ shows that $c E_{bp}$ becomes zero, i.e., the craze becomes complete plastic material, such a matter is not encountered in practice. That is, before becoming completely plastic, the craze cracks and fractures. $\phi_p = 1$ shows a specimen filled with only the craze or the matrix.

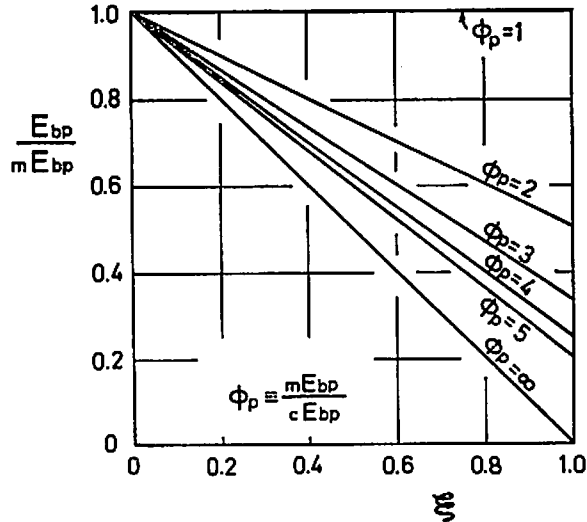


Fig. 16 $E_{bp}/m E_{bp}$ vs. ξ

2. Bending in Direction Perpendicular to Major Axis Craze

A schematic bending specimen model in the direction perpendicular to the major axis of the craze as shown in Fig. 17 is discussed. It is assumed that: the matrix and the craze are arranged at equal intervals from each other; their number are respectively n_b ; quantity of the craze is ζ ; bending elastic modulus of the matrix is ${}_m E_{bv}$; bending elastic modulus of the craze is ${}_c E_{bv}$; thickness of specimen is t ; width of specimen is w ; and length of specimen is l . If a bending specimen in the direction perpendicular to the major axis of the craze is given pure bending moment M_b , strain energy occurs. For a sandwich structure specimen which is constituted with crazes and matrices as shown Fig. 17, assuming the radii of curvature at respective boundaries of the craze and matrix to be equal, the relationship between M_b and

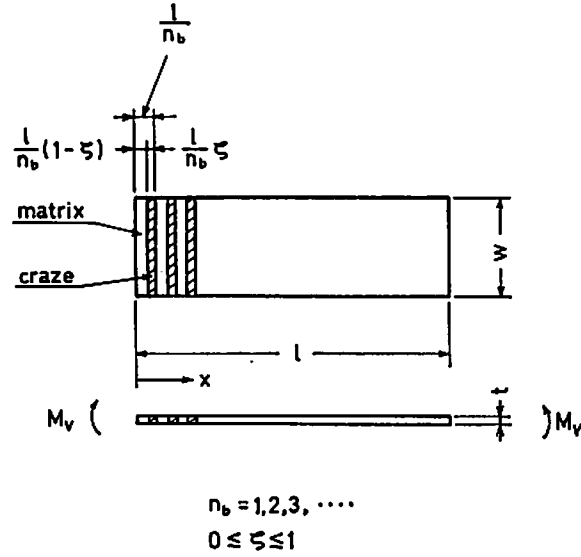


Fig. 17 Schematic bending specimen model in direction perpendicular to major axis of craze.

strain energy U is:

$$U = \frac{n_b}{2} \left\{ \int_0^{l/n_b(1-\xi)} \frac{M_v^2}{mE_{bv} mI_v} dx + \int_0^{l/n_b\xi} \frac{M_v^2}{cE_{bv} cI_v} dx \right\} \quad (5)$$

where mI_v is the geometrical moment of inertia of the matrix and cI_v is the geometrical moment of inertia of the craze. In Eq. (5), if M_v , mE_{bv} , cE_{bv} , mI_v and cI_v can be assumed to be independent of x , Eq. (5) can be integrated to:

$$U = \frac{lM_v^2}{2} \left\{ \frac{1}{mE_{bv} mI_v} (1-\xi) + \frac{1}{cE_{bv} cI_v} \xi \right\} \quad (6)$$

If, in place of the sandwich structure specimen a unitary structure having elastic modulus E_{bv} and geometrical moment of inertia I_v is used, U of the unitary structure is:

$$U = \frac{lM_v^2}{2E_{bv} I_v} \quad (7)$$

The following expression is obtained from Eqs. (6) and (7):

$$E_{bv} = \frac{1}{I_v} \frac{mE_{bv} cE_{bv} mI_v cI_v}{cE_{bv} cI_v (1-\xi) + mE_{bv} mI_v \xi} \quad (8)$$

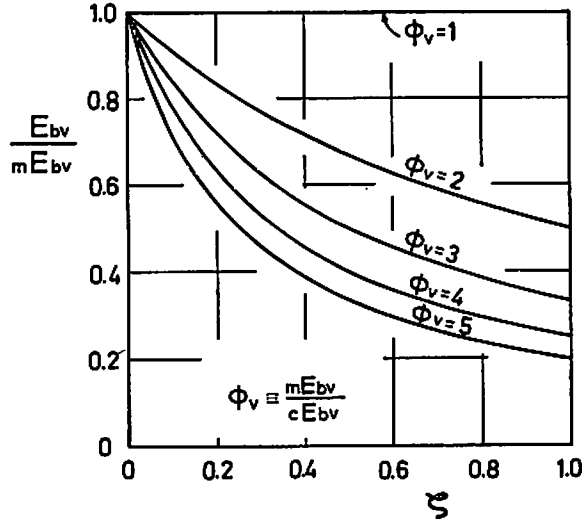
If sectional shapes of the matrix and the craze can be assumed to be equal, thus $mI_v = cI_v \equiv I_v$, Eq. (8) simplifies to:

$$\frac{E_{bv}}{mE_{bv}} = \frac{1}{1 + (\phi_v - 1)\xi}, \quad \phi_v \equiv \frac{mE_{bv}}{cE_{bv}} \quad (9)$$

The relationship between E_{bv}/mE_{bv} and ξ is shown in Fig. 18. This graph shows that the relationship between E_{bv}/mE_{bv} and ξ is curvilinear. $\phi_v = 1$ shows a specimen filled with only the craze or the matrix.

3. Anisotropy under Bending

Anisotropy defined as E_{bp}/E_{bv} is obtained from ratio of Eqs. (4) and (9).


 Fig. 18 E_{bv}/mE_{bv} vs. ζ

The ratio is:

$$\frac{E_{bp}}{E_{bv}} = \{mE_{bp}(1-\xi) + cE_{bp}\xi\} \left\{ \frac{cE_{bv}(1-\zeta) + mE_{bv}\zeta}{mE_{bv}cE_{bv}} \right\} \quad (10)$$

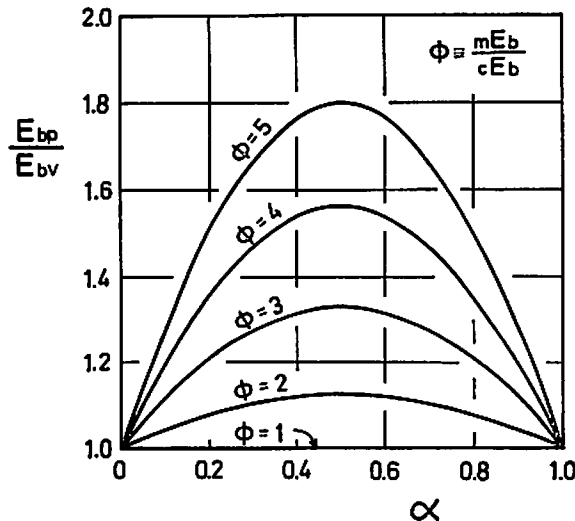
If $mE_{bp} = mE_{bv} = mE_b$ and $cE_{bp} = cE_{bv} = cE_b$ can be assumed, however, cE_{bp} may not be practically equal to cE_{bv} , Eq. (10) simplifies to:

$$\frac{E_{bp}}{E_{bv}} = \left\{ 1 + \left(\frac{1}{\phi} - 1 \right) \xi \right\} \left\{ 1 + (\phi - 1)\zeta \right\}, \quad \phi \equiv \frac{mE_b}{cE_b} \quad (11)$$

When $\xi = \zeta \equiv \alpha$ is, from Eq. (11), the following result is obtained:

$$\frac{E_{bp}}{E_{bv}} = \left\{ 1 + \left(\frac{1}{\phi} - 1 \right) \alpha \right\} \left\{ 1 + (\phi - 1)\alpha \right\} \quad (12)$$

The relationship between E_{bp}/E_{bv} and α is shown in Fig. 19. There is an interesting point in this graph: at $\alpha = 0.5$, i.e., quantity of the craze is 50%, E_{bp}/E_{bv} has maximum value and increases with increase in ϕ . $\alpha = 0$ indicates to be zero quantity of


 Fig. 19 E_{bp}/E_{bv} vs. α

the craze, i.e., to be zero quantity of the stress-whitening. $\alpha=1$ indicates that quantity of the craze is 100%.

V. Discussion

In Fig. 9, the bending strength at 100°C is extremely small in comparison with the value at temperatures lower than 90°C. This phenomenon indicates that the glass transition temperature is in between 90°C and 100°C. Fig. 12 shows that the bending strength increases in straight line with increase in temperature at tensile load. This can be understood from the fact that the quantity of stress-whitening of the specimen tends to decrease as the temperature increases, as shown in Fig. 8. The specimen extracted from the tensed specimen at 100°C proved to have the same strength as the matrix. This phenomenon shows that stress-whitening and anisotropy do not occur when the tensed specimen is over the glass transition temperature.

In the repeating test for bending and eliminating of the stress-whitening, as shown in Fig. 13, a crack occurs when the number of times for bending is in the neighbourhood of 16. Until a crack occurs, the bending strength stays at a constant value regardless of the number of times for bending and the strength is the same as the matrix's. This phenomenon seems to correspond to the fatigue phenomenon of metal.

When measured with a microwave 9375 MHz, the values of dielectric constant of the matrix and of the stress-whitened specimen differ hardly at all. The dielectric constant of the specimens extracted in respective directions from the tensile specimen as shown in Fig. 14 also differ little from the value of the matrix. These observations seem to imply that the method of measurement used was not accurate, because different values of dielectric constant are actually thought to exist. By utilizing more severe measure method, consequently, their values of the specimens may be measured.

It is evident that the bending strength employed in the experiments is related functionally to the bending elastic modulus used in theoretical analyses. It will require greatly effort to obtain more the experimental data in great various testing conditions. The mechanical strength properties estimated with extensive measure condition can be analogized from the theoretical results. That is, the bending strength in the experiments and the elastic modulus in theoretical analyses can not be compared directly, but the mutual relationship can be analogized. For instance, looking at Figs. 10 and 19, anisotropy defined as S_t/S_n in Fig. 10 increases in straight line with increase in the tensile strain (quantity of the stress-whitening); however anisotropy defined as E_{bp}/E_{bv} in Fig. 19 changes parabolically. These things seem to correspond as follow: the data in Fig. 10 corresponds to merely part of the data in Fig. 19; where α and ϕ in Fig. 19 are smaller, a thought that the relationship between E_{bp}/E_{bv} and α is linear is approximately correct. The material in which crazing or stress-whitening occurred was assumed in this paper to be elastic, however, actually, high polymer material is viscoelastic. Therefore, discussions of viscoelastic transactions will be prospectively tried.

Acknowledgement

We would like to thank Mr. Seitaro Nishiki in Mitsui-Toatsu Kagaku Co., Ltd., Prof. Yoshio Hirata, Prof. Kimio Kawakita, Prof. Noriomi Ochiai and Mr. Makoto Tsutsui in our laboratory for valuable discussion. We are much indebted to Mitsui-Toatsu Kagaku Co., Ltd. for supplying materials.

Nomenclature

- E_{bp} = elastic modulus of sandwich structure specimen shown in Fig. 15. (kg/mm²)
 E_{bv} = elastic modulus of sandwich structure specimen shown in Fig. 17. (kg/mm²)
 ${}_cE_{bp}$ = bending elastic modulus of the craze shown in Fig. 15. (kg/mm²)
 ${}_cE_{bv}$ = bending elastic modulus of the craze shown in Fig. 17. (kg/mm²)
 ${}_mE_{bp}$ = bending elastic modulus of the matrix shown in Fig. 15. (kg/mm²)
 ${}_mE_{bv}$ = bending elastic modulus of the matrix shown in Fig. 17. (kg/mm²)
 I_p = geometrical moment of inertia of sandwich structure specimen shown in Fig. 15. (mm⁴)
 I_v = geometrical moment of inertia of sandwich structure specimen shown in Fig. 17. (mm⁴)
 ${}_cI_p$ = geometrical moment of inertia of the craze shown in Fig. 15. (mm⁴)
 ${}_cI_v$ = geometrical moment of inertia of the craze shown in Fig. 17. (mm⁴)
 ${}_mI_p$ = geometrical moment of inertia of the matrix shown in Fig. 15. (mm⁴)
 ${}_mI_v$ = geometrical moment of inertia of the matrix shown in Fig. 17. (mm⁴)
 k_b = respective number which the matrix and craze in Fig. 15 are arranged at equal intervals from each other. (dimensionless)
 l = distance between fulcrums in bending test. (mm)
 l = length of specimen shown in Fig. 17. (mm)
 M_p = pure bending moment shown in Fig. 15. (kgm)
 M_v = pure bending moment shown in Fig. 17. (kgm)
 n_b = respective number which the matrix and craze in Fig. 17 are arranged at equal intervals from each other. (dimensionless)
 P = maximum load in bending load-deflection curve. (kg)
 S = bending strength. (kg/mm²)
 S_{\perp} = bending strength of specimen in direction perpendicular to tensile stress. (kg/mm²)
 S_{\parallel} = bending strength of specimen in direction of tensile stress. (kg/mm²)
 t = thickness of bending specimen. (mm)
 U = strain energy. (kgm)
 w = width of bending specimen. (mm)
 x = rectangular coordinate, direction perpendicular to the major axis of craze, Fig. 17.
 α = value for $\xi = \zeta$, i.e., $\xi = \zeta \equiv \alpha$.
 ζ = quantity of the craze shown in Fig. 17. (dimensionless)
 ξ = quantity of the craze shown in Fig. 15. (dimensionless)
 ρ = radius of curvature resulted by M_p . (mm)
 $\phi = {}_mE_b / {}_cE_b$. (dimensionless)
 $\phi_p = {}_mE_{bp} / {}_cE_{bp}$. (dimensionless)
 $\phi_v = {}_mE_{bv} / {}_cE_{bv}$. (dimensionless)

References

- 1) O.K. Spurr & W.D. Niegish, J. Appl. Polym. Sci., **6**, 585 (1962).
- 2) J. A. Sauer, J. Marin & C.C. Hsiao, J. Appl. Phys., **20**, 507₁(1949).
- 3) C.C. Hsiao & J. A. Sauer, J. Appl. Phys., **21**, 1071 (1950).
- 4) K. Ito, Kobunshi no Bussei to Seikei-Kako, 229.
- 5) M. Matsuo, Japan Plastics, **3**, 7 (1967).
- 6) C.B. Bucknall & R.R. Smith, Polymer, **6**, 437 (1965).
- 7) R.P. Kambour, Appl. Polym. Symp., **7**, 215 (1968).

- 8) R.P. Kambour, *Polym. Engg. and Sci.*, 4, 281 (1968).
- 9) C.G. Montgomery, *Technique of Microwave Measurements*, Vol. 11, 561.
- 10) M. Kasajima, K. Ito & S. Koido, *Nippon Kikai Gakkai-Rombunshu*, 700-12, 249 (1970).
- 11) M. Kasajima, K. Ito & S. Koido, 21th Sosei Kako Rengokoenkai-Rombunshu, 491 (1970).